Technical University of Denmark

DTU

Spin Structures in Magnetic Nanoparticles

Mørup, Steen; Brok, Erik; Frandsen, Cathrine

[Link to publication](#)

Review Article

Spin Structures in Magnetic Nanoparticles

Steen Mørup,[1] Erik Brok,[1,2] and Cathrine Frandsen[1]

[1] *Department of Physics, Technical University of Denmark, 2800 Kongens Lyngby, Denmark*
[2] *Center for Electron Nanoscopy, Technical University of Denmark, 2800 Kongens Lyngby, Denmark*

Correspondence should be addressed to Cathrine Frandsen; fraca@fysik.dtu.dk

Spin structures in nanoparticles of ferrimagnetic materials may deviate locally in a nontrivial way from ideal collinear spin structures. For instance, magnetic frustration due to the reduced numbers of magnetic neighbors at the particle surface or around defects in the interior can lead to spin canting and hence a reduced magnetization. Moreover, relaxation between almost degenerate canted spin states can lead to anomalous temperature dependences of the magnetization at low temperatures. In ensembles of nanoparticles, interparticle exchange interactions can also result in spin reorientation. Here, we give a short review of anomalous spin structures in nanoparticles.

1. Introduction

The magnetic properties of nanoparticles differ in many respects from those of the corresponding bulk materials [1]. In very small magnetic particles, the magnetization direction is not fixed but fluctuates at finite temperatures, and the magnetization may spontaneously be reversed (superparamagnetic relaxation) above the blocking temperature [2, 3]. At low temperatures, the spin wave excitations are dominated by the uniform mode ($q = 0$ spin waves), resulting in a linear temperature dependence of the magnetization in contrast to the Bloch $T^{3/2}$ law valid for bulk materials [4]. In several studies, it has been found that the saturation magnetization of nanoparticles of ferrimagnetic materials is smaller than the bulk value. This can in many cases be explained by spin canting, that is, noncollinear spin structures. The reduced number of magnetic neighbor ions around surface atoms can lead to magnetic frustration, which results in canted spin structures in materials with otherwise collinear spin structures [5, 6]. Near the surface, the low local symmetry can result in a large contribution to the local magnetic anisotropy, which also can influence the spin orientations. Both in nanoparticles and in bulk materials, defects in the interior, such as diamagnetic substitution or cation vacancies, can also lead to noncollinearity [7]. In materials with spin canting there may be different canted states that are separated by very low energy barriers [7]. Therefore, magnetic fluctuations can take place at very low temperatures. Freezing of the spins can result in an anomalous temperature dependence of the magnetization at low temperatures. Moreover, exchange interaction between surface atoms of neighboring particles can have a profound influence on the magnetic properties because this can affect both the superparamagnetic relaxation [8–10] and the spin structure [9, 11]. For many applications of magnetic nanoparticles, a large saturation magnetization is desirable, and it is therefore important to control and minimize spin canting. In this paper, we present a short review on spin structures in magnetic nanoparticles.

2. Theoretical Models for Spin Canting

Canted spin structures at surfaces and around defects in the interior of a material are in general very complex, and analytical calculations of the magnetic properties may therefore not be feasible, but the spin structures can be elucidated by use of computer simulations. Kodama et al. [12] have performed computer simulations of the spin structure of 2.5 nm nanoparticles of the inverse spinel $NiFe_2O_4$. In the simulations, the magnetic anisotropy was neglected and it was assumed that the interior of the particles was defect-free. Therefore, there is only spin canting near the surface. Figure 1 shows a calculated spin structure for a (111) plane
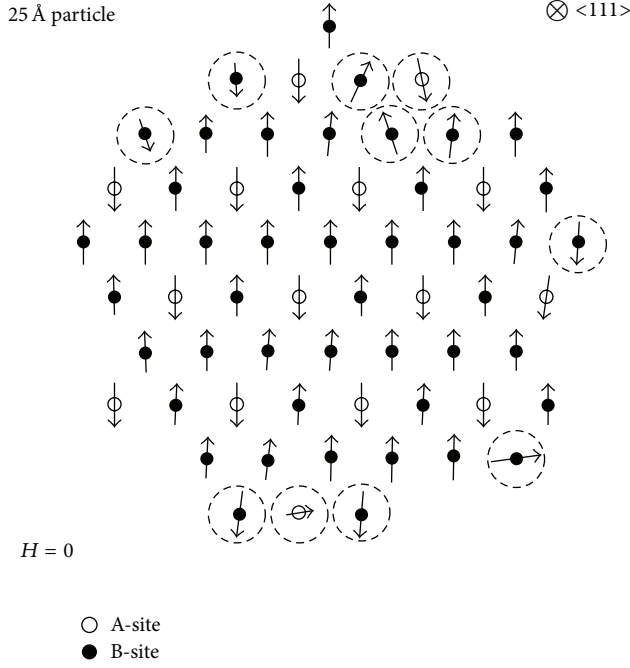
FIGURE 1: Calculated spin structures for a (111) cross-section of a 2.5 nm NiFe$_2$O$_4$ particle. Reproduced with permission from Kodama et al. [12].
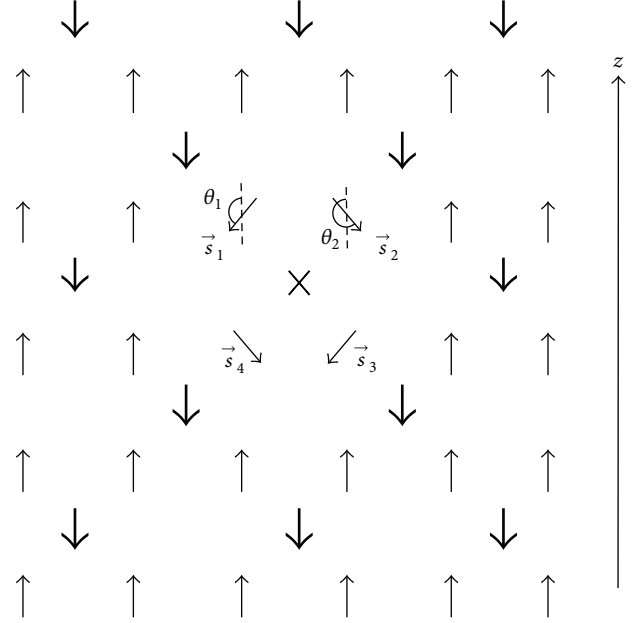

FIGURE 2: Schematic illustration of a canted two-dimensional spin structure. The bold arrows correspond to A-site spins and the other arrows correspond to B-site spins. The cross represents a missing A-site spin. Reproduced with permission from Jacobsen et al. [14].

of a 2.5 nm NiFe$_2$O$_4$ particle. Highly misoriented spins are indicated by dashed circles. It is noteworthy that some of the surface spins are completely reversed. The simulations also showed that different canted states commonly are separated by very low energy barriers. If surface anisotropy is included in the model, more surface spins will be strongly canted [13].

In very simple cases, analytical calculations of spin structures around defects and at surfaces can be performed. Although simple, these calculations show at least qualitatively that the magnetization may increase or decrease in an anomalous way at low temperatures. Figure 2 shows a simple two-dimensional canted spin structure, which allows obtaining analytical solutions for the spin directions and the temperature dependence of the magnetization by use of a classical model [7, 14]. In the model, spins at A-sites and B-sites are antiparallel in the defect-free structure. The bold arrows in Figure 2 represent A-site spins and the remaining arrows represent B-site spins. The cross represents a missing A-site spin, which can give rise to magnetic frustration and canting of neighboring B-site spins. In the calculations, the magnetic anisotropy and canting of next nearest spins are neglected. For symmetry reasons, the angles between the spins and the z-direction are assumed to be pairwise identical. The magnetic energy can then be written [7, 14]:

$$E\left(\theta_1, \theta_2\right) = a\left(\cos\theta_1 + \cos\theta_2\right) + b\cos\left(\theta_1 - \theta_2\right), \quad (1)$$

where θ_1 and θ_2 are defined in the figure, $a = 4\lambda_{BB} - 2\lambda_{AB} + 2\lambda_L - 2\mu B$, and $b = 4\lambda_{BB}$. Here, λ_{BB} is the exchange parameter for nearest neighbor B-B coupling, λ_{AB} is the exchange parameter for nearest neighbor A-B coupling, and λ_L is the exchange parameter for the exchange interaction between a

B-site ion and all more distant ions. μ is the magnetic moment of a B-site ion, and B is the applied magnetic field, defining the z-direction.

By differentiating (1), one can find the spin orientations, which give minimum energy. Calculations have been performed for $b/k_B = 200$ K (k_B is Boltzmann's constant) and values of a/b between 1.1 and 1.9 [14]. Energy minima are found for $\sin\theta_1 = -\sin\theta_2$ and $\cos\theta_1 = \cos\theta_2 = -a/2b$ with energy $E_{\min} = -b - a^2/2b$. They are separated by maxima at $\theta_1 = \theta_2 = 180°$ with $E(180°, 180°) = -2a + b$. A more comprehensive discussion of the energy maxima and minima in simple canted spin structures is given in [7].

For arbitrary values of θ_1, the values of θ_2, which minimize the energy, are given by [14]

$$tg\theta_2 = \frac{b\sin\theta_1}{a + b\cos\theta_1}, \quad (2)$$

and the magnetic energy as a function of the angle θ_1 is given by [14]

$$E\left(\theta_1\right) = a\cos\theta_1 - \sqrt{a^2 + b^2 + 2ab\cos\theta_1}. \quad (3)$$

Figure 3 shows the magnetic energy as a function of θ_1 for values of a/b between 1.1 and 1.9. At very low temperatures, the system is found in an energy minimum, but at higher temperatures, the spin may perform transverse relaxation, that is, fluctuations of the spin directions across the energy barrier at $\theta_1 = 180°$. For $1.7 \leq a/b < 2.0$, the height of the energy barrier is less than 10 K, and transverse relaxation may therefore take place at very low temperatures.

In general, the average value of the z component of the magnetic moment is given by $\langle M^z(T)\rangle = 2\mu\langle\cos\theta_1 + \cos\theta_2\rangle$,
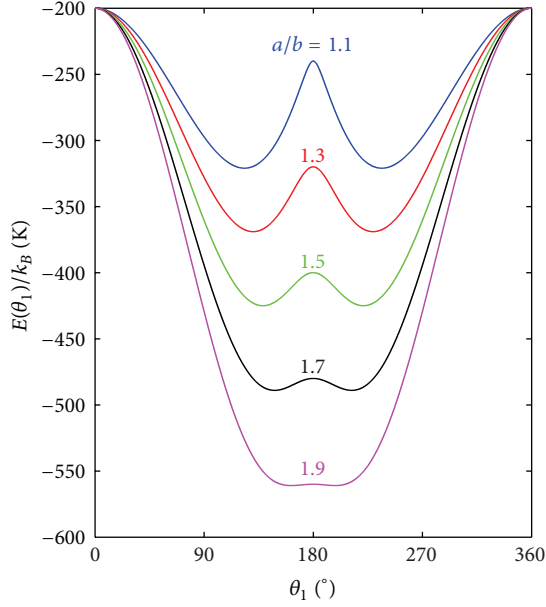
FIGURE 3: The energy of the canted spin structure, shown in **Figure 2**, as a function of the angle θ_1 for the indicated values of a/b. The calculations were carried out using (3) with $b/k_B = 200$ K. Reproduced with permission from Jacobsen et al. [14].
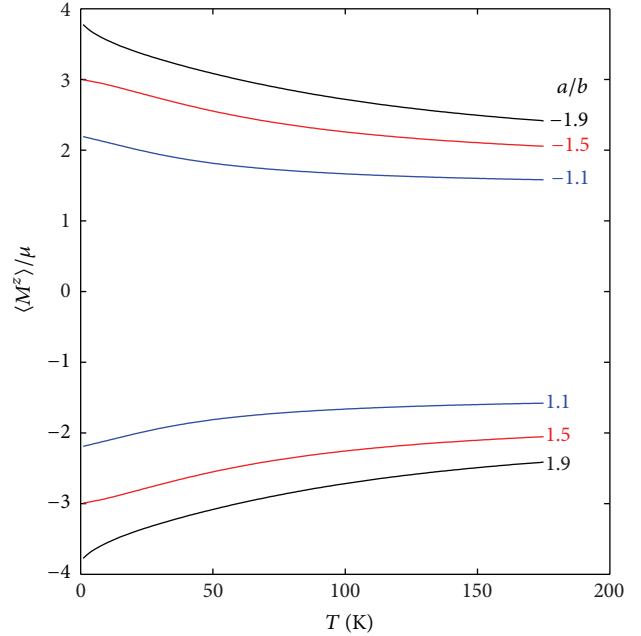

FIGURE 4: Temperature dependence of the thermal average of the canted spin structure, shown in **Figure 2**. The calculations were carried out using Boltzmann statistics for $b/k_B = 200$ K and the indicated values of a/b. Reproduced with permission from Jacobsen et al. [14].

where μ is the magnetic moment of a single atom. The temperature dependence of $\langle M^z(T) \rangle$ for values of a/b between 1.1 and 1.9 and between -1.1 and -1.9 calculated by use of Boltzmann statistics is shown in **Figure 4**. At low temperatures, the thermal average of the magnetic moment increases or decreases rapidly with decreasing temperature. Several experimental studies of ferrimagnetic nanoparticles have shown anomalous temperature dependencies of the magnetization at low temperatures that are in accordance with this model [12, 17–24]. A quantum mechanical calculation gives results that are qualitatively similar to those of the classical model [14].

3. Experimental Studies of Spin Canting

Mössbauer spectroscopy in large applied magnetic fields is a very useful method to investigate spin canting in ferrimagnetic materials [5, 6]. The magnetic hyperfine splitting in Mössbauer spectra is proportional to the total magnetic field at the nucleus, B_{tot}, which has contributions from the hyperfine field, B_{hf}, and the applied field, B_{app}, and can be found from the relationship

$$B_{hf}^2 = B_{tot}^2 + B_{app}^2 - 2 B_{tot} B_{app} \cos \theta, \tag{4}$$

where θ is the angle between the direction of the total magnetic field at the nucleus and the gamma ray direction. The relative areas of the six lines of a ^{57}Fe Mössbauer spectrum of a magnetic material depend on the angle θ as the relative areas are given by $3 : p : 1 : 1 : p : 3$, where

$$p = \frac{4 \sin^2 \theta}{2 - \sin^2 \theta}. \tag{5}$$

In polycrystalline ferrimagnetic materials in zero applied field with random orientation of the crystallites, the orientations of the sublattice magnetization directions are random, and the relative areas are then $3 : 2 : 1 : 1 : 2 : 3$. If a large magnetic field is applied parallel to the gamma ray direction, the sublattice magnetization directions of a collinear ferrimagnetic material will be parallel and antiparallel to this direction, resulting in zero intensity of lines 2 and 5. However, in nanoparticles of ferrimagnetic materials, these two lines usually have nonzero intensity because of spin canting. In several publications, it has been suggested that this spin canting is located at the surface, because the reduced number of magnetic neighbor ions at the surface can result in magnetic frustration. However, in other studies it has been found that the canting does not vary with particle size in a regular way [25–27]. This strongly suggests that canting is not only a surface effect but also commonly occurs around defects in the interior of the particles [25–27].

As an example, **Figure 5** shows a Mössbauer spectrum of magnetic Dynabeads, consisting of $1 \, \mu$m porous polymer beads containing 7.7 nm maghemite (γ-Fe$_2$O$_3$) particles in the pores. Such beads are used, for example, for preparation and handling of biological materials, and a large saturation magnetization of the maghemite particles is essential for the performance. The saturation magnetization of the maghemite particles in the beads was 336 kA m^{-1} [28], which is about 10% less than the bulk value. The Mössbauer spectrum, shown in **Figure 5**, was obtained at 6.0 K with a magnetic field of 6.0 T applied parallel to the gamma ray direction. The spectrum

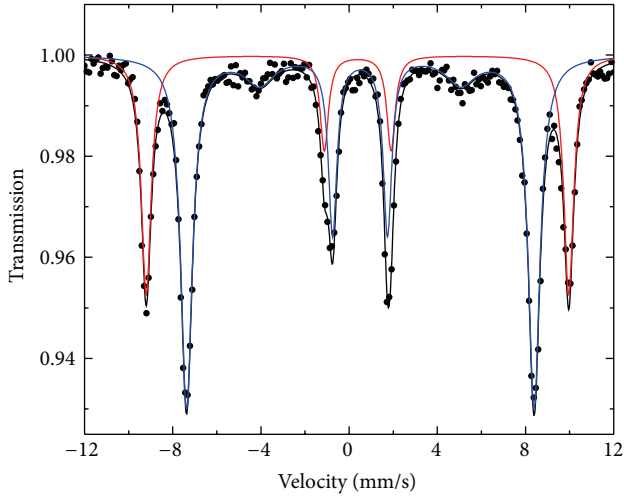Figure 5: Mössbauer spectrum of $1\,\mu$m magnetic Dynabeads, containing 7 nm maghemite (γ-Fe$_2$O$_3$) nanoparticles. The spectrum was obtained at 6 K with a magnetic field of 6 T applied parallel to the gamma ray direction. The red and blue fit lines represent Fe^{3+} in A- and B-sites, respectively.

was fitted with two sextets, corresponding to iron in the A-sites (red fit lines) with a total field of 59.4 T and B-sites (blue fit lines) with a total field of 48.9 T. The intensity of lines 2 and 5 of the A-site component is negligible, whereas the relative areas of lines 2 and 5 for the B-site component were $p \approx 0.55$, corresponding to an average canting angle, $\theta \approx 29°$ for the B-site spins. These results show that there is essentially no canting in A-sites but some canting in B-sites. The canting can affect all B-site ions or be restricted to a fraction of B-site spins with large canting angles, but the data can explain at least qualitatively the reduced value of the saturation magnetization compared to the bulk value.

A study of the temperature dependence of the spin structure has been made for 7 nm maghemite particles [15]. The Mössbauer spectra of the sample, shown in Figure 6, were obtained at the indicated temperatures with a magnetic field of 4 T applied parallel to the gamma ray direction. At low temperatures, lines 2 and 5 have nonzero intensity indicating the presence of spin canting. The best fits of the spectra were obtained with three sextets, two of which had zero intensity of lines 2 and 5, corresponding to iron in the tetrahedral A-and the octahedral B-sites of the spinel structure with a perfect collinear ferrimagnetic structure. The third sextet with nonzero intensity of lines 2 and 5 had an isomer shift indicating that it was mainly due to iron in the octahedral B-sites. Thus, the data indicate that the canting only affects a fraction of the B-site spins, whereas the remaining B-site spins and the A-site spins are essentially not affected by the canting. Sextets 1 and 2 had relatively narrow lines at all temperatures, but sextet 3 showed a substantial line broadening and a decreasing relative area of lines 2 and 5 with increasing temperature. Similar results have been found in studies of 2.7 nm and 4.6 nm maghemite particles [29]. This temperature dependence can be explained by transverse relaxation between canted states, characterized by canting
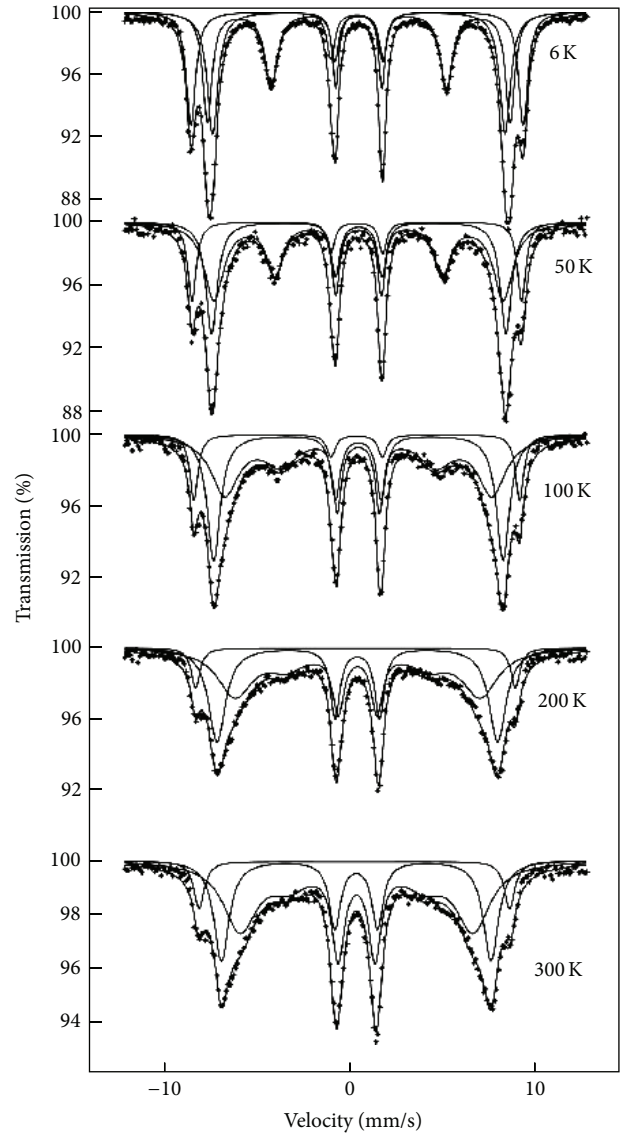

Figure 6: Mössbauer spectra of 7.7 nm maghemite (γ-Fe$_2$O$_3$) particles. The spectra were obtained at the indicated temperatures with a magnetic field of 4 T applied parallel to the gamma ray direction. Reproduced with permission from Helgason et al. [15].

angles θ_c and $-\theta_c$. At very low temperatures, the spins are fixed in one of two energy minima (curves plotted in Figure 3 for the simple canted structure shown in Figure 2). When the temperature is increased, relaxation takes place between the two minima and this results in line broadening, and for very fast relaxation, the nucleus only experiences the average field that is parallel (or antiparallel) to the applied field and the gamma ray direction. Similar data have been found in studies of diamagnetically substituted bulk ferrimagnets such as Mn$_{0.25}$Zn$_{0.75}$Fe$_2$O$_4$ [30] and Li$_{1.125}$Ti$_{1.25}$Fe$_{0.625}$O$_4$ [31].

When the transverse relaxation is fast, the magnitude of the average hyperfine field will be given by $B_0\langle\cos\theta\rangle$. The fits of the spectra in Figure 6 show that the relative intensity of lines 2 and 5 of sextet 3 does not disappear completely even
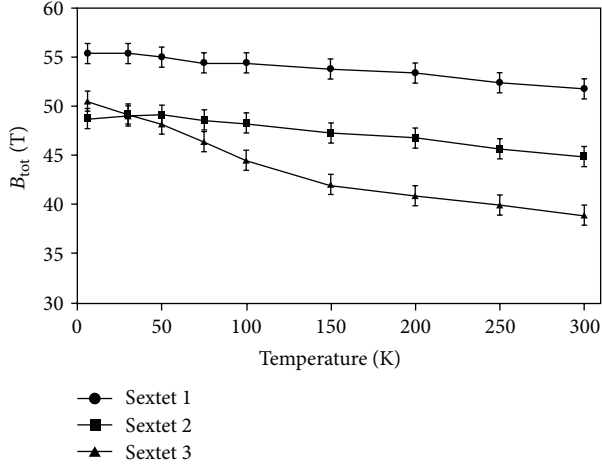
FIGURE 7: Temperature dependence of the total magnetic field at the nuclei, obtained from fits of the spectra shown in Figure 6. Reproduced with permission from Helgason et al. [15].

at 300 K indicating relaxation times of the same order of magnitude as the time scale of Mössbauer spectroscopy. The temperature dependence of the magnetic hyperfine fields of the three sextets is shown in Figure 7. For sextets 1 and 2, the hyperfine fields decrease by a few percent when heating up to 300 K. This is similar to the behavior of bulk maghemite. However, the hyperfine field of sextet 3 decreases much faster with increasing temperature, in accordance with the model for transverse relaxation of the canted spins and the overall temperature dependence of the particle magnetization.

4. Spin Reorientation due to Interparticle Interactions

Magnetic interactions between nanoparticles can have a large influence on the magnetic properties. Magnetic dipole interactions between ferromagnetic or ferrimagnetic nanoparticles can significantly affect the superparamagnetic relaxation time [10]. Nanoparticles of antiferromagnetic particles usually have a finite magnetic moment because of uncompensated spins, but this moment is typically so small that the dipole interactions are insignificant [8]. However, if antiferromagnetic nanoparticles are in close proximity, the superparamagnetic relaxation can be suppressed because of exchange interactions between surface atoms of neighboring particles [8, 10]. Such exchange interactions can in some cases also have a strong influence on the spin structure [9, 11, 16]. This can conveniently be investigated by Mössbauer spectroscopy studies. In hematite (α-Fe$_2$O$_3$) nanoparticles, the magnitude and the sign of the quadrupole shift depend on the angle θ_0 between the [001] direction of the hexagonal structure and the magnetic hyperfine field. The quadrupole shift is given by [11]

$$\varepsilon = \frac{\varepsilon_0 \left(3\cos^2\theta_0 - 1\right)}{2}, \tag{6}$$

where $\varepsilon_0 = 0.20$ mm/s. In bulk hematite, $\theta_0 = 0°$ below the Morin transition temperature at $T \approx 263$ K, whereas $\theta_0 = 90°$ above this temperature, such that $\varepsilon = -0.10$ mm/s. However, in noninteracting hematite nanoparticles with dimensions below ~20 nm, $\theta_0 = 90°$ at all temperatures, but interparticle interactions can change the spin orientation [11]. In a recent study of α-Fe$_2$O$_3$/NiO nanocomposites [16], it was found that interactions between the hematite and nickel oxide nanoparticles can have a very strong influence on the spin orientation in the hematite nanoparticles. Figure 8(a) shows Mössbauer spectra of noninteracting 8 nm hematite particles, and Figure 8(b) shows Mössbauer spectra of hematite nanoparticles from the same batch, but interacting with NiO nanoparticles. At the lowest temperatures, the difference in quadrupole shift of the hematite nanoparticles in the two samples is easily measurable. Fitting the spectra of noninteracting hematite nanoparticles (Figure 8(a)) provides a spin angle of $\theta_0 = 90°$ for all particles. The spectra of the hematite nanoparticles interacting with NiO (Figure 8(b)) were well fitted with two sextets. The quadrupole shifts of the two sextets as a function of temperature are shown in Figure 9. For sextet 1, the quadrupole shift is around + 0.16 mm/s corresponding to $\theta_0 = 21°$, whereas sextet 2 has a quadrupole shift of 0.08 mm/s corresponding to $\theta_0 = 39°$. This clearly shows that the spin angle deviates significantly from that of noninteracting particles where $\theta_0 = 90°$, but we note that the bimodal distribution of spin angles ($\theta_0 = 21°$, $\theta_0 = 39°$) may be a consequence of the fitting procedure using only two sextets. With increasing temperature, the quadrupole shifts of both sextets decrease; that is, the spin angle θ_0 increases. Neutron diffraction studies of the samples confirmed the Mössbauer data and furthermore found that the spin angle is the same within each particle (i.e., no domain formation) [16].

The data can be at least qualitatively understood by considering the interaction between the two particles shown in Figure 10. The magnetic energy of the two particles may be written as

$$E\left(\theta_p, \theta_q\right) = K_p V_p \sin^2\theta_p + K_q V_q \sin^2\theta_q \\ - J_{\text{eff}} M_p M_q \cos\left(\alpha - \theta_p - \theta_q\right). \tag{7}$$

The first two terms represent the anisotropy energies of particles p and q, respectively, where K_p and K_q are the anisotropy constants, V_p and V_q the volumes, and θ_p and θ_q the angles between the sublattice magnetizations and the easy axes of the particles. The last term comes from the effective exchange interaction between the particles p and q where J_{eff} is the exchange coupling constant between the sublattice magnetizations, M_p and M_q, of the particles p and q, and α denotes the angle between the easy axes $\vec{e}_p$ and $\vec{e}_q$. Because of the exchange interaction at the interface, the sublattice magnetization directions $\vec{M}_p$ and $\vec{M}_q$ are rotated by the angles θ_p and θ_q, respectively. For an arbitrary value of θ_p the minimum energy is found for

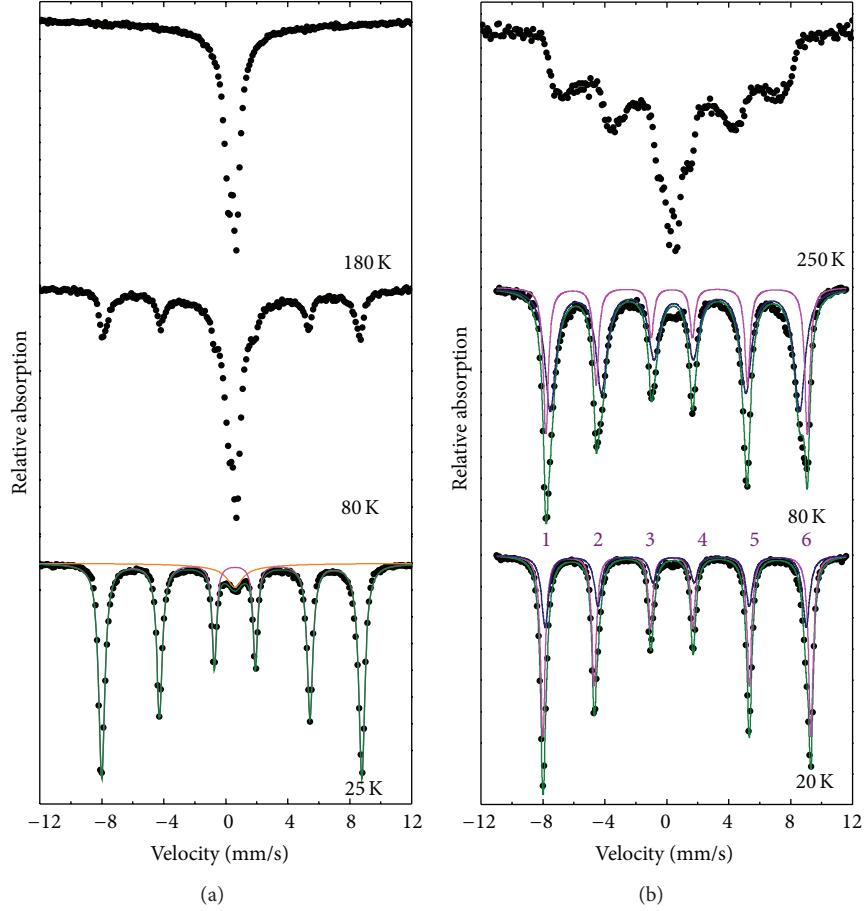$$\sin 2\theta_q = \frac{K_p V_p}{K_q V_q} \sin 2\theta_p. \tag{8}$$

FIGURE 8: Mössbauer spectra of 8 nm hematite (α-Fe$_2$O$_3$) nanoparticles obtained at the indicated temperatures. (a) Noninteracting hematite particles coated with oleic acid and in aqueous suspension. (b) Hematite particles mixed with NiO. The spectra of the α-Fe$_2$O$_3$/NiO nanocomposite were fitted with two sextets, as shown in panel (b). Reproduced with permission from Frandsen et al. [16].
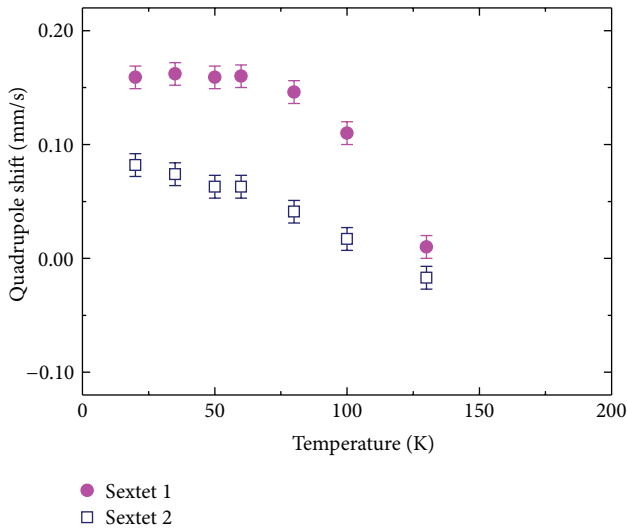

FIGURE 9: Temperature dependence of the quadrupole shift of the two sextet components shown in Figure 8(b). Reproduced with permission from Frandsen et al. [16].

To illustrate the effects of interactions, we here consider the simple case where $K_p V_p = K_q V_q \equiv KV$ for which one can find an analytical solution for the rotation angle $\theta_p = \theta_q \equiv \theta_r$

$$\cot 2\theta_r = \frac{KV}{E_{\text{int}} \sin \alpha} + \cot \alpha, \qquad (9)$$

where $E_{\text{int}} = J_{\text{eff}} M_p M_q$. If the easy axes of the two particles are parallel ($\alpha = 0°$), one finds that $\theta_r = 0°$ irrespective of the strength of the interaction energy. However, a large interaction energy compared to the anisotropy in combination with a large value of the angle α results in a large rotation angle, θ_r, at low temperatures. At higher temperatures, the sublattice magnetization directions perform fast fluctuations around the directions corresponding to the energy minima [1, 8, 10]. Therefore, M_p and M_q should be replaced by the thermal averages $\langle M_p \rangle$ and $\langle M_q \rangle$ such that the interaction energy is given by $E_{\text{int}} = J_{\text{eff}} \langle M_p \rangle \langle M_q \rangle$. With increasing temperature, $\langle M_p \rangle$ and $\langle M_q \rangle$ decrease leading to an increase of $\cot 2\theta_r$, that is, a decrease of the spin rotation angle. Such a mechanism
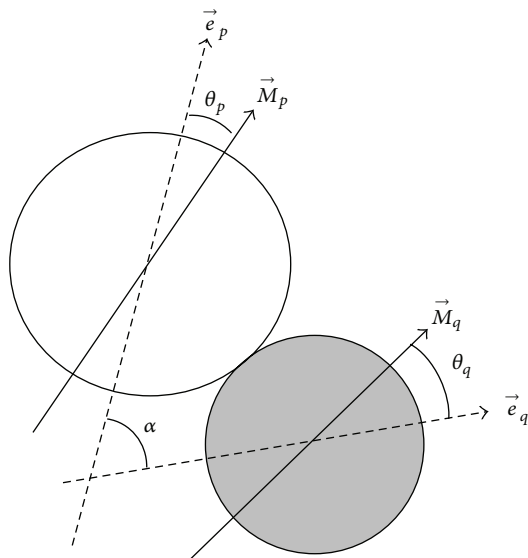
FIGURE 10: Schematic illustration of two interacting nanoparticles with easy axes $\vec{e}_p$ and $\vec{e}_q$ and sublattice magnetization directions $\vec{M}_p$ and $\vec{M}_q$. α is the angle between the two easy axes, and θ_p and θ_q denote the angles between the easy axes and the sublattice magnetization of the two particles. Reproduced with permission from Frandsen et al. [16].

can qualitatively explain the temperature dependence of the reorientation angle.

Also, in samples of interacting hematite particles, a spin reorientation has been observed, but the effect is smaller than that in the α-Fe$_2$O$_3$/NiO nanocomposite [11].

5. Conclusions

Theoretical and experimental studies of magnetic nanoparticles show that the spin structures often differ from those of perfect bulk materials. The low symmetry around surface atoms and around defects in the interior of the particles can lead to localized spin canting, and also thermal fluctuations between almost degenerate spin states may take place even at low temperature. This can lead to anomalous magnetization behaviors of nanoparticles. Furthermore, exchange interactions between surface atoms of neighboring nanoparticles in close proximity can result in reorientation of the sublattice magnetization directions in the whole particles.

Conflict of Interests

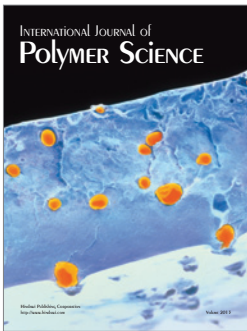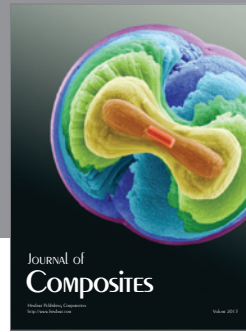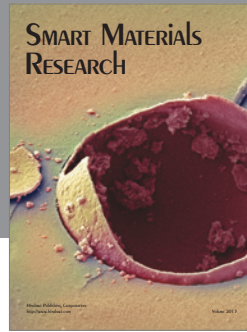The authors declare no conflict financial of interests.

References

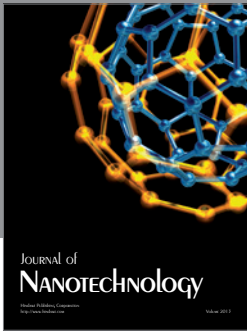[1] S. Mørup, M. F. Hansen, and C. Frandsen, "Magnetic nanoparticles," in *Comprehensive Nanoscience and Technology*, D. Andrews, G. Scholes, and G. Wiederrecht, Eds., vol. 1, pp. 437–491, Elsevier, 2011.

[2] L. Néel, "Théorie du traînage magnétique des ferromagnétiques en grains fins avec applications aux terres cuites," *Annales Geophysique*, vol. 5, pp. 99–136, 1949.

[3] W. F. Brown, "Thermal fluctuations of a single-domain particle," *Physical Review*, vol. 130, p. 1677, 1963.

[4] S. Mørup, C. Frandsen, and M. F. Hansen, "Uniform excitations in magnetic nanoparticles," *Beilstein Journal of Nanotechnology*, vol. 1, pp. 48–54, 2010.

[5] J. M. D. Coey, "Noncollinear spin arrangement in ultrafine ferrimagnetic crystallites," *Physical Review Letters*, vol. 27, pp. 1140–1142, 1971.

[6] A. H. Morrish and K. Haneda, "Surface magnetic properties of fine particles," *Journal of Magnetism and Magnetic Materials*, vol. 35, p. 105, 1983.

[7] S. Mørup, "Spin-canting and transverse relaxation at surfaces and in the interior of ferrimagnetic particles," *Journal of Magnetism and Magnetic Materials*, vol. 266, p. 110, 2003.

[8] M. F. Hansen, C. Bender Koch, and S. Mørup, "Magnetic dynamics of weakly and strongly interacting hematite nanoparticles," *Physical Review B*, vol. 62, p. 1124, 2000.

[9] C. Frandsen and S. Mørup, "Inter-particle interactions in composites of antiferromagnetic nanoparticles," *Journal of Magnetism and Magnetic Materials*, vol. 266, p. 36, 2003.

[10] S. Mørup, M. F. Hansen, and C. Frandsen, "Magnetic interactions between nanoparticles," *Beilstein Journal of Nanotechnology*, vol. 1, p. 182, 2010.

[11] C. Frandsen and S. Mørup, "Spin rotation in α-Fe$_2$O$_3$ nanoparticles by interparticle interactions," *Physical Review Letters*, vol. 94, Article ID 027202, 2005.

[12] R. H. Kodama, A. E. Berkowitz, E. J. McNiff Jr., and S. Foner, "Surface spin disorder in NiFe$_2$O$_4$ nanoparticles," *Physical Review Letters*, vol. 77, no. 2, pp. 394–397, 1996.

[13] R. H. Kodama and A. E. Berkowitz, "Atomic-scale magnetic modeling of oxide nanoparticles," *Physical Review B*, vol. 59, p. 6321, 1999.

[14] H. Jacobsen, K. Lefmann, E. Brok, C. Frandsen, and S. Mørup, "Temperature dependence of the magnetization of canted spin structures," *Journal of Magnetism and Magnetic Materials*, vol. 324, p. 3218, 2012.

[15] Ö. Helgason, H. K. Rasmussen, and S. Mørup, "Spin-canting and transverse relaxation in maghemite nanoparticles and in tin-doped maghemite," *Journal of Magnetism and Magnetic Materials*, vol. 302, p. 413, 2006.

[16] C. Frandsen, K. Lefmann, B. Lebech et al., "Spin reorientation in α-Fe$_2$O$_3$ nanoparticles induced by interparticle exchange interactions in α-Fe$_2$O$_3$/NiO nanocomposites," *Physical Review B*, vol. 84, Article ID 214435, 2011.

[17] E. Tronc, A. Ezzir, R. Cherkaoui et al., "Surface-related properties of γ-Fe$_2$O$_3$ nanoparticles," *Journal of Magnetism and Magnetic Materials*, vol. 221, p. 63, 2000.

[18] H. Kachkachi, A. Ezzir, M. Nogués, and E. Tronc, "Surface effects in nanoparticles: application to maghemite γ-Fe$_2$O$_3$," *The European Physical Journal B*, vol. 14, p. 681, 2000.

[19] T. N. Shendruk, R. D. Desautels, B. W. Southern, and J. van Lierop, "The effect of surface spin disorder on the magnetism

of γ-Fe$_2$O$_3$ nanoparticle dispersions," *Nanotechnology*, vol. 18, no. 45, Article ID 455704, 2007.

[20] F. T. Parker, M. W. Foster, D. T. Margulies, and A. E. Berkowitz, "Spin canting, surface magnetization, and finite-size effects in γ-Fe$_2$O$_3$ particles," *Physical Review B*, vol. 47, no. 13, pp. 7885–7891, 1993.

[21] K. Mandal, S. Mitra, and P. A. Kumar, "Deviation from Bloch T3/2 law in ferrite nanoparticles," *Europhysics Letters*, vol. 75, no. 4, pp. 618–623, 2006.

[22] D. Peddis, C. Cannas, G. Piccaluga, E. Agostinelli, and D. Fiorani, "Spin-glass-like freezing and enhanced magnetization in ultra-small CoF$_2$O$_4$ nanoparticles," *Nanotechnology*, vol. 21, no. 12, Article ID 125705, 2010.

[23] C. N. Chinnasamy, A. Narayanasamy, N. Ponpandian et al., "Mixed spinel structure in nanocrystalline NiFe$_2$O$_4$," *Physical Review B*, vol. 63, no. 18, Article ID 184108, 2001.

[24] B. Martinez, X. Obradors, L. Balcells, A. Rouanet, and C. Monty, "Low temperature surface spin-glass transition in γ-Fe$_2$O$_3$ nanoparticles," *Physical Review Letters*, vol. 80, p. 181, 1997.

[25] C. J. Serna, F. Bødker, S. Mørup, M. P. Morales, F. Sandiumenge, and S. Veintemillas-Verdaguer, "Spin frustration in maghemite nanoparticles," *Solid State Communications*, vol. 118, no. 9, pp. 437–440, 2001.

[26] S. Chkoundali, S. Ammer, N. Jouini et al., "Nickel ferrite nanoparticles: elaboration in polyol medium via hydrolysis, and magnetic properties," *Journal of Physics: Condensed Matter*, vol. 16, p. 4357, 2004.

[27] A. G. Roca, D. Niznansky, J. Poltierova-Vejpravova et al., "Magnetite nanoparticles with no surface spin canting," *Journal of Applied Physics*, vol. 105, no. 11, Article ID 114309, 2009.

[28] G. Fonnum, C. Johansson, A. Molteberg, S. Mørup, and E. Aksnes, "Characterisation of Dynabeads (R) by magnetization measurements and Mössbauer spectroscopy," *Journal of Magnetism and Magnetic Materials*, vol. 293, p. 41, 2005.

[29] E. Tronc, P. Prené, J. P. Jolivet, J. L. Dormann, and G. M. Grenèche, "Spin canting in γ-Fe$_2$O$_3$ nanoparticles," *Hyperfine Interactions*, vol. 112, p. 97, 1998.

[30] T. A. Anhøj, B. Bilenberg, B. Thomsen et al., "Spin canting and magnetic relaxation phenomena in Mn$_{0.25}$Zn$_{0.75}$Fe$_2$O$_4$," *Journal of Magnetism and Magnetic Materials*, vol. 260, p. 115, 2003.

[31] J. L. Dormann, M. El Harfaoui, M. Noguès, and J. Jove, "Relaxation of the transverse spin component in randomly canted Li-Ti ferrite below T$_N$," *Journal of Physics C*, vol. 20, p. L161, 1987.